**ANALYSIS OF CALCIUM SULFATE-CEMENTED SANDSTONES AND VEINS ALONG THE MSL TRAVERSE, GALE CRATER, MARS**, A. M. Baker[1], G. E. Ganter[1], M. A. Nellessen[1], H. E. Newsom[1], R. S. Jackson[1], M. Nachon[2], F. Rivera-Hernandez[2], J. Williams[1], R. C. Wiens[4], J. Frydenvang[4], P. Gasda[4], N. Lanza[4], A. Ollila[4], S. Clegg[4], O. Gasnault[5], S. Maurice[5], P.-Y. Meslin[5], A. Cousin[5], W. Rapin[6], J. Lasue[5], O. Forni[5], J. L'Haridon[5], D. Blaney[6], V. Payré[7], N. Mangold[8], L. LeDeit[8], R. Anderson[9], [1]U. New Mexico, Albuquerque, NM 87131, USA (allisonmbaker@unm.edu); [2]UC Davis, CA;; [4]Los Alamos Nat. Lab, NM; [5]IRAP/CNRS, FR; [6]Caltech/Jet Prop. Lab, CA; [7]U. Lorraine de Nancy, FR; [8]Lab. de Planet. et Geodynam. de Nantes, FR; [9]USGS, Flagstaff, AZ.

**Introduction:** The Mars Science Laboratory Rover Curiosity has observed abundant calcium sulfate veins in all the bedrock examined to date in Gale Crater, except for the Bradbury Rise or Rocknest Outcrop areas. Recently in the upper Murray, ChemCam analysis of light-toned rocks have suggested the presence of a cemented porous sandstone with moderate Ca and S. The ChemCam analyses normally consist of 30 laser shots, with the first 5 shots omitted from the average value to avoid dust contamination [2]. To further investigate the nature of the targets, we have used ChemCam shot to shot data to evaluate the heterogeneity of Ca-S bearing targets that may represent cement, veins, and other depositional features.

**Detection of calcium sulfate cement:** In sandstone, typical porosities vary between 5% by volume up to ~ 30% by volume, with poorly sorted materials having less pore space. Therefore, the relative maximum for pore-filling cement is around 30 wt% for Ca-sulfate [1]. Pure Ca-sulfate veins tend to contain Ca in abundance of around 35-45 wt%. Thus, CaO abundances around 20 wt% would be consistent with a cemented sandstone.

Cemented sandstones have very homogeneous shot-to-shot trends with a low standard deviation (<2.0 wt %). We compiled all the shot-to-shot data from targets averaging 10 to 25 wt% CaO, and found that approximately 80% of the targets with moderate CaO exhibited a homogeneous trend, and that most targets with intermediate CaO represent cemented rocks and not the edge of a vein. This has been verified by Mastcam context imagery. We then examined more closely the targets displaying heterogeneous shot to shot patterns, which we call special targets.

**Analysis of shot to shot data for special targets:** We have begun looking at the shot-to-shot patterns to determine different classifications for types of targets we are hitting. These patterns include flat-trending, continuous increasing or decreasing, concave increasing or decreasing, and several irregular and complex patterns. Understanding and theorizing the potential causes of different shot-to-shot patterns may allow us to determine possibilities for what type of targets each pattern represents and use this information to learn about the environment the feature was deposited in.

The flat-trending or straight targets may be indicative of a homogenized material, such as would be expected of a cement that permeated into empty pore space (**Fig. 1**). This is the most common patterned encountered among the moderate CaO targets (**Fig. 6**).

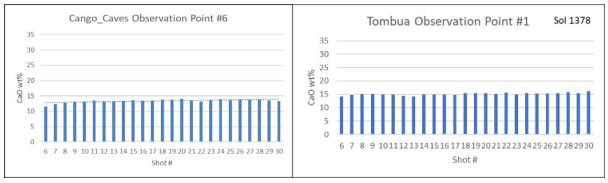


**Fig. 1 A.** Cango_Caves Observation Point #6 (sol 1876) shows a flat trend at an average of 13.3 wt % CaO and a standard deviation of 0.54 wt % CaO. **B.** Tombua Observation Point #1 shows a flat trend as well with an average of 15.2 wt % CaO and a standard deviation of 0.47 wt % CaO.

The steady increasing and decreasing targets indicate progressive change from the top to the bottom of the shot profile. Instances in which this would occur would be if the laser hit the vein at an oblique angle and the profile is slowly transitioning from vein into bedrock (Thunderbolt target, **Fig. 2 A.**) or vice versa. The laser could also be encountering an increasing/decreasing concentration of cement (Zuluand_ccam, **Fig. 2 B.**). The steady increasing or decreasing profile is the second most common among the heterogeneous targets (**Fig. 6**).

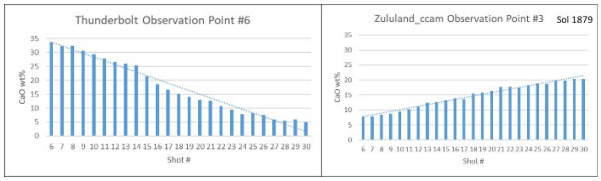


**Fig. 2 A.** Thunderbolt Observation Point #6 (sol 1033) is a heterogeneous target that shows a decreasing trend with a slope of -1.3342 and a standard deviation of 9.96 wt % CaO. **B.** Zululand_ccam Observation Point #3 is a heterogeneous target that shows an increasing trend with a slope of 0.57 and a standard deviation of 4.3 wt % CaO.

The concave up and concave down targets demonstrate a more rapid increase of CaO in a short time

span. These targets may represent a target that is mostly cement or bedrock but transitions rapidly at either the beginning or end of the profile, or it may represent variabilities in the cement concentration. This profile is relatively uncommon among the heterogeneous targets (**Fig. 6**).

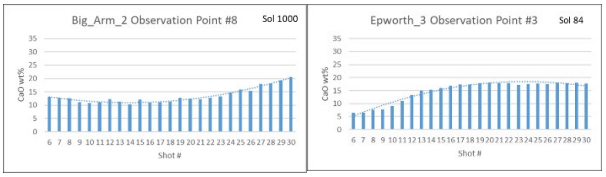


**Fig. 3 A.** Big_Arm_2 Observation Point #8 shows a concave/convex up trend with a standard deviation of 2.8 wt % CaO. **B.** Epwort_3 Observation Point #3 shows a concave/convex down trend with a standard deviation of 4.2 wt % CaO.

Irregular patterns have sharp changes or nonlinear trends (**Fig. 4**). We suspect that this occurs in one of 3 ways: when the laser hits an irregular mix of Ca-sulfate cement and bedrock, it hits Ca-sulfate grains embedded within the bedrock, or it hits thin Ca-sulfate veins filling in the cracked bedrock**.** It is the most common pattern observed among the heterogeneous targets (**Fig. 6)**.

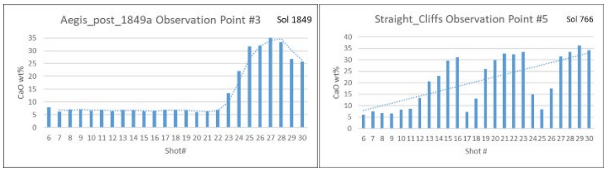


**Fig. 4 A.** Aegis_post_1849a Observation Point #3 shows a homogeneous trend with a sharp increase at shot 23. This observation point has a standard deviation of 10.1 wt % CaO. **B.** Straight_Cliffs Observation Point #5 shows extreme variation in wt % with a standard deviation of 11.2 wt % CaO.

Complex patterns are relatively flat or gently increasing/decreasing trends with slight variations in wt % that form bimodal or trimodal peaks (**Fig. 5**). This could be the result of variance in layering of the Ca-sulfate cements or a variance in abundance of Ca-sulfate particles within the bedrock. Complex patterns are also uncommon trends for heterogeneous targets to show (**Fig. 6**).

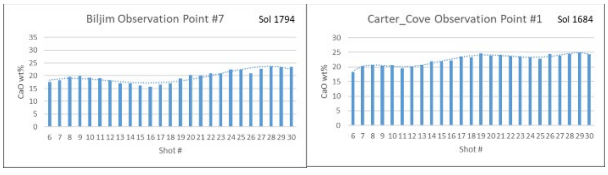


**Fig. 5 A.** Biljim Observation Point #7 shows a bimodal complex pattern with a standard deviation of 0.63 wt % CaO and an average of 25.1 wt % CaO. **B.** Carter_cove Observation Point #1 shows a trimodal complex pattern with a standard deviation of 1.87907 wt % CaO and an average of 23 wt % CaO.

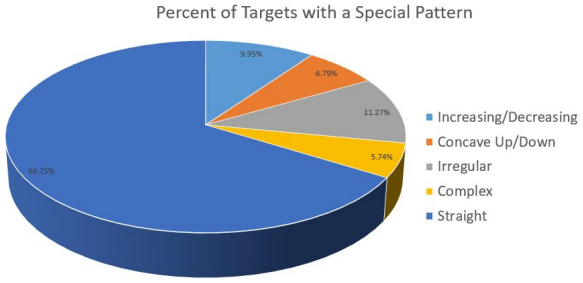


**Fig. 6** As visible by the pie chart, straight/flat targets are the most common (66.3%) followed by irregular (11.3%), increasing/decreasing (9.95%), concave/convex (6.79%), and complex (5.74%).

**Special Shot to Shot Patterns in Relation to Grain Sizes:** The diameter of the laser is very small (350-500 µm in diameter FWIW); and the depth of penetration even smaller, only ~0.3-0.4 µm/pulse in basalt, and closer to ~1-2 µm/pulse in a sandy dolomite as found by Lanza et al. [3]. Since the fine sand grain size class is from 125 – 250 µm, homogenous mixtures of materials smaller than this should have a relatively constant shot to shot pattern, even if the individual grains are different in composition. If the grains (or the edge of a vein partly intercepted by the beam) are approaching the medium sand size (250 – 500 µm), the shot to shot data could vary as seen in some of the patterns. For the homogeneous cement targets, we do not see this, therefore we can conclude that even if the grains are larger than the laser beam, they are all the same composition. Further analysis could be conducted concerning special patterns and if they have any significant relation to grain sizes in heterogeneous targets. A network of homogeneously distributed tiny Ca-S veins, less than a few tens of microns could explain the data, but such an occurrence could be considered to be one type of cement.

**Conclusions:** We have confirmed the likely presence of Ca-S cement (interpenetrating a silicate matrix) in many ChemCam analyses using the typical 25 dust free shots on each target point. To further our investigation of the nature of these special patterns and targets, we are looking for correlations between the special targets and their characteristics in the ChemCam RMI and MastCam imagery.

**References:** [1] Newsom et al. 2016 LPSC, and 2017 LPSC, and in preparation. [2] Lasue, J. et al., (2018). Martian eolian dust probed by ChemCam. *Geophysical Research Letters*. [3] Lanza et al., (2015) Icarus.